

Characterization of Nonanuclear Europium and Gadolinium Complexes by Gas-Phase Luminescence Spectroscopy

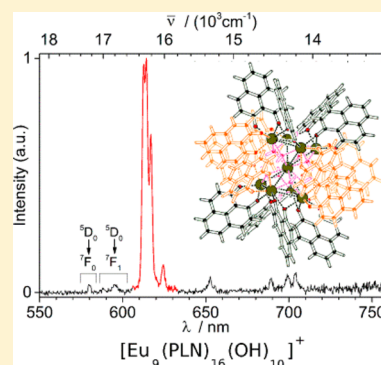
Jean-François Greisch,^{*,†} Michael E. Harding,[†] Bernhard Schäfer,[†] Mario Ruben,[†] Wim Klopper,^{†,‡} Manfred M. Kappes,^{†,‡} and Detlef Schooss^{*,†,‡}

[†]Institute of Nanotechnology, Karlsruhe Institute of Technology (KIT), Hermann-von-Helmholtz-Platz 1, 76344 Eggenstein-Leopoldshafen, Germany

[‡]Institute of Physical Chemistry, Karlsruhe Institute of Technology (KIT), Fritz-Haber-Weg 2, 76131 Karlsruhe, Germany

S Supporting Information

ABSTRACT: Gas-phase measurements using mass-spectrometric techniques allow determination of the luminescence properties of selected molecular systems with knowledge of their exact composition. Furthermore, isolated luminophores are unaffected by matrix effects like solvent interactions or crystal packing. As a result, the system complexity is reduced relative to the condensed phase and a direct comparison with theory is facilitated. Herein, we report the intrinsic luminescence properties of nonanuclear europium(III) and gadolinium(III) 9-hydroxyphenalen-1-one (HPLN)–hydroxo complexes. Luminescence spectra of $[\text{Eu}_9(\text{PLN})_{16}(\text{OH})_{10}]^+$ ions reveal an europium-centered emission dominated by a 4-fold split Eu(III) hypersensitive transition. The corresponding Gd(III) complex, $[\text{Gd}_9(\text{PLN})_{16}(\text{OH})_{10}]^+$, shows a broad emission from a ligand based triplet state with an onset of about 1000 wavenumbers in excess of the europium emission. As supported by photoluminescence lifetime measurements for both complexes, we deduce an efficient europium sensitization via PLN-based triplet states. The luminescence spectra of the complexes are discussed in terms of a square antiprismatic europium/gadolinium core structure as suggested by density functional computations.



SECTION: Spectroscopy, Photochemistry, and Excited States

The high processability and cost effectiveness of lanthanoid coordination complexes make them attractive materials for a broad range of applications extending from light emitting diodes¹ and plastic optical fiber amplifiers² to memory devices.³ Some applications are affected by lanthanoid-specific restrictions. For example, the extremely low absorption cross sections of the 4f–4f transitions of lanthanoid cations hinder their direct optical excitation. For others such as time-resolved bioassays, UV excitation is best avoided due to the strong absorption of shorter wavelengths by nucleic acids, aromatic amino acids, and reduced pyridine nucleotides.⁴ In such cases, lanthanoid sensitization is best achieved via intramolecular energy transfer from efficiently visible light absorbing antennas complexed to the weakly absorbing emitters. If the specific spectroscopic properties of the free lanthanoid ions are mostly retained upon antenna complexation, they can nevertheless be fine-tuned via a close control of the ions' coordination shells.⁵ Herein, effective sensitization of Eu(III) was achieved by making use of the advantageous light harvesting properties of the deprotonated 9-hydroxyphenalen-1-one ligand (PLN[−]) allowing effective sensitization at wavelengths extending from the UV into the visible region.⁶

This work is part of a systematic study of the intrinsic properties of photoluminescent ionic chromophores in the gas phase using mass spectrometric and, in particular, ion trapping techniques.^{7,8} Inherent to this approach is the knowledge of the

exact stoichiometry of the noncovalent or coordination complexes studied. Compared with condensed-phase measurements where the exact stoichiometry is often not known or regulated by equilibria, it also provides information on the impact of the environment on the properties of the investigated systems.

Our interest is presently focused on stable and discrete polynuclear complexes because such systems may exhibit new functions that depend on intermetallic communications.^{9–12} Polynuclear lanthanoid–oxo/hydroxo complexes obtained by ligand-controlled hydrolysis of a lanthanoid salt are particularly interesting in this regard. In the present Letter, we contrast the photophysical properties of the structurally similar $[\text{Eu}_9(\text{PLN})_{16}(\text{OH})_{10}]^+$ and $[\text{Gd}_9(\text{PLN})_{16}(\text{OH})_{10}]^+$ complexes, each of which uses the light-harvesting properties of PLN ligands to different advantage.

$[\text{Eu}_9(\text{PLN})_{16}(\text{OH})_{10}]\text{Cl}$ and $[\text{Gd}_9(\text{PLN})_{16}(\text{OH})_{10}]\text{Cl}$ were synthesized as detailed in the Supporting Information. The experimental setup used is described in ref 13, with a short overview provided in the Supporting Information.

Received: March 28, 2014

Accepted: May 1, 2014

Published: May 1, 2014

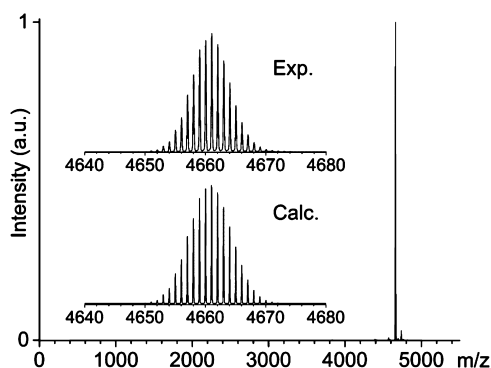


Figure 1. ESI mass spectrum in positive ion mode of the $[\text{Eu}_9(\text{PLN})_{16}(\text{OH})_{10}]^+$ complex sprayed from a dichloromethane solution (SYNAPT G2S HDMS, Waters).

An ESI mass spectrum of the europium compound is shown in Figure 1. Photoluminescence measurements were performed on the cation corresponding to the stoichiometry of $[\text{Eu}_9(\text{PLN})_{16}(\text{OH})_{10}]^+$. The compound probed in the gas phase was completely free from contaminations due to smaller nuclearities. Ion mobility measurements performed on $[\text{Eu}_9(\text{PLN})_{16}(\text{OH})_{10}]^+$ using a separate setup (see Supporting Information) revealed no indication of multiple isomers.

Structural information about $[\text{Eu}_9(\text{PLN})_{16}(\text{OH})_{10}]^+$ was inferred from density functional computations. The X-ray crystal structure determined for a similarly synthesized $[\text{Tb}_9(\text{PLN})_{16}(\text{OH})_{10}]^+$ complex was used as the starting point for the corresponding structure optimization (to be published separately). Specifically, all solvent molecules were removed from the unit cell and Tb(III) was replaced by Eu(III). The optimization was performed without symmetry restrictions using the B-P functional¹⁴ in combination with the def2-SVP basis set^{15,16} employing the TURBOMOLE program package.¹⁷ The resolution-of-identity (RI) approximation was applied in all ground-state energy calculations.^{15,18} The *xyz* coordinates of the structure are provided as Supporting Information.

The resulting structure is shown in Figure 2. The $(\text{Eu}(\text{III}))_9$ core is hourglass-shaped with the central Eu(III) cation in a square-antiprismatic coordination environment, a structural motif well known for nonanuclear hydroxo-lanthanoid complexes.^{19–25} $[\text{Eu}_9(\text{PLN})_{16}(\text{OH})_{10}]^+$ has two different Eu(III) coordination sites (see Figure 2). The central Eu(III) occupies a highly symmetric ($\sim D_{4d}$) site, whereas the remaining eight Eu(III) ions are located on low local symmetry sites ($\sim C_{2v}$). Two sorts of PLN^- ligands are distinguishable: eight pairwise stacked terminal ligands form a belt around $(\text{Eu}(\text{III}))_9$ core, each binding to a Eu(III) cation in either the top or the bottom of the hourglass core; the remaining eight PLN^- are almost perpendicularly oriented with respect to each other and bind two adjacent metal ions on the same square face at the top and bottom of the hourglass $(\text{Eu}(\text{III}))_9$ core. Adjacent europium ions in both square faces are also linked by one μ_4 -OH moiety, and each triangular face is additionally capped by another μ_3 -OH group.

The gas-phase luminescence spectrum of $[\text{Eu}_9(\text{PLN})_{16}(\text{OH})_{10}]^+$ shown in Figure 3 reveals the characteristic metal centered emission bands $^5D_0 \rightarrow ^7F_0$ ($17\,240\text{ cm}^{-1}$), $^5D_0 \rightarrow ^7F_1$ ($16\,920\text{ cm}^{-1}$), $^5D_0 \rightarrow ^7F_2$ ($16\,010$ – $16\,320\text{ cm}^{-1}$) $^5D_0 \rightarrow ^7F_3$ ($15\,320\text{ cm}^{-1}$) and $^5D_0 \rightarrow ^7F_4$ ($14\,350\text{ cm}^{-1}$), dominated by the hypersensitive $^5D_0 \rightarrow ^7F_2$ band. The weak

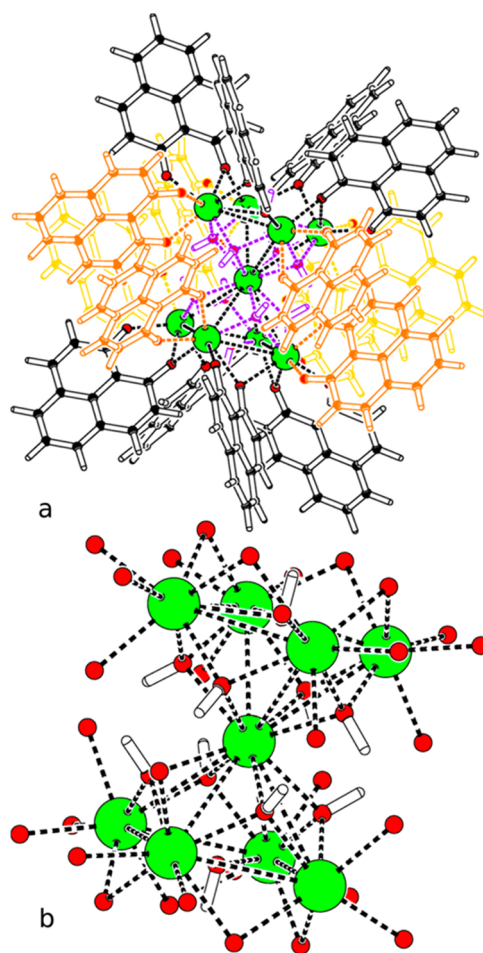


Figure 2. (a) Molecular structure of the $[\text{Eu}_9(\text{PLN})_{16}(\text{OH})_{10}]^+$ ion computed at the RI-B-P/def2-SVP level: stacked terminal ligands forming a belt around the ion center (orange), bridging ligands (black), and hydroxyl groups (violet). (b) $(\text{Eu}(\text{III}))_9^+$ core (green) with the first coordination shell (red oxygens).

nondegenerate $^5D_0 \rightarrow ^7F_0$ transition at $17\,240\text{ cm}^{-1}$ can be indicative of the number of differently coordinated Eu(III) ions.²⁶ This feature is unimodal at the resolution of the measurement, even though the cluster has two different Eu(III) sites. The pseudo- D_{4d} symmetry of the central Eu(III) however leads to symmetry-forbidden $^5D_0 \rightarrow ^7F_0$ and $^5D_0 \rightarrow ^7F_2$ transitions²⁷ and, therefore, this central cation does not contribute to these transitions (to first order). Consequently, the strong hypersensitive band $^5D_0 \rightarrow ^7F_2$ originates from the eight outer Eu(III) ions. The intensity ratio of the $^5D_0 \rightarrow ^7F_2$ transition to the $^5D_0 \rightarrow ^7F_0$ transition is found to be about 20. Even if efficient sensitization of the central Eu(III) occurred and a deviation from D_{4d} symmetry took place, its contribution would nevertheless be diluted in those of the eight outer europium ions. The $^5D_0 \rightarrow ^7F_2$ transition comprises four well-separated subbands starting at $16\,010\text{ cm}^{-1}$ with splittings on the order of 300 cm^{-1} , even though five subbands are expected for C_{2v} sites. Because our experimental resolution is limited, the fifth band may be hidden or too weak to be detected. Note that the total number of observed bands for the hypersensitive transition is another indication of the presence of a single isomer. Overall, the number of subbands, as well as their intensity distribution, is in good agreement with the suggested structure.

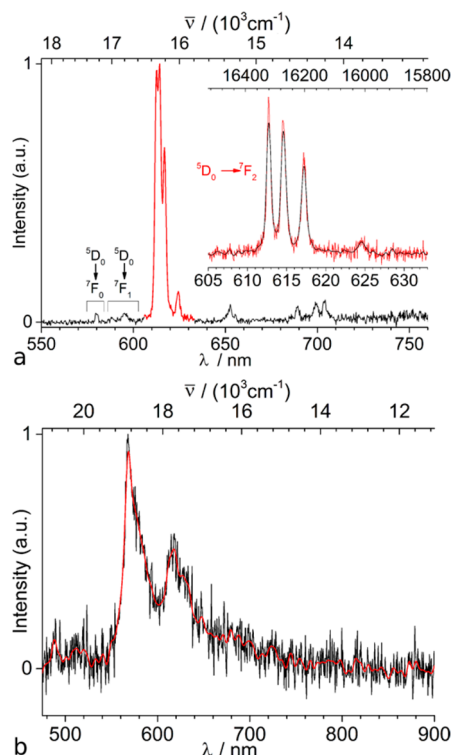


Figure 3. Luminescence spectra of (a) $[\text{Eu}_9(\text{PLN})_{16}(\text{OH})_{10}]^+$ (55 W/cm², 476.5 nm, 83 K, corrected) with the hypersensitive band measured at a higher resolution (inset) and (b) $[\text{Gd}_9(\text{PLN})_{16}(\text{OH})_{10}]^+$ (1975 W/cm², 476.5 nm excitation, 83 K).

The high quality of the gas-phase $[\text{Eu}_9(\text{PLN})_{16}(\text{OH})_{10}]^+$ luminescence spectrum suggests that the energy transfer from the ligands to the europium centers is highly efficient. The generally accepted sensitization pathway for Eu(III) complexes involves the excitation of a ligand-based singlet state followed by intersystem crossing into a ligand-based triplet state, which is succeeded by a resonant energy transfer to levels belonging to an excited state centered on an europium ion. For this mechanism to be efficient, the ligand-centered donating level needs to be nearly equal or slightly above the emitting level of the lanthanide ion to prevent energy back-transfer to the ligand-based triplet manifold.^{28,29} Other possible mechanisms include a direct energy transfer from a ligand based excited singlet state to the energy levels of the europium ion, although the short lifetime of the singlet excited state typically prevents efficient energy transfer,^{30–32} or a direct photoexcitation of a ligand based triplet state (with an extremely low probability) followed by energy transfer to the lanthanoid ion.³³

A way to probe the energy of the ligand-based levels and to assess the likelihood of their involvement is to measure the phosphorescence spectrum of the analogous Gd(III) compound.^{34–36} Gd(III) cannot provide an appropriate acceptor state for antennas in the near-UV/vis range because its first excited state ($^6\text{P}_{7/2}$) lies $\sim 32\,000\text{ cm}^{-1}$ above its ground state. Hence, the chemical similarity of Gd(III) and Eu(III)—their ionic radii differ by less than 1%—allows the study of intraligand phosphorescence for a ligand topology very close to that of the actual Eu(III) complex. The measurement performed on $[\text{Gd}_9(\text{PLN})_{16}(\text{OH})_{10}]^+$ shows a strong emission band extending from about 550 to 620 nm (Figure 3b) and is attributed to phosphorescence from the lowest triplet state T_1 of the ligand. A more detailed explanation, that is, of the

observed structured emission with peaks at $\sim 16\,270$ and $17\,610\text{ cm}^{-1}$, requires further measurements and computations also of homologues containing different numbers of Ln(III) ions and PLN[−] ligands. These go beyond the scope of this Letter. We note that such structure may reflect the two topologically different PLN[−] ligands or may be caused by excitonic states, indicating strongly coupled ligands.^{37–40} The emission onset is at $\sim 18\,200\text{ cm}^{-1}$, $\sim 960\text{ cm}^{-1}$ above the $^5\text{D}_0$ emission level of Eu(III) but also $\sim 1000\text{ cm}^{-1}$ lower than its $^3\text{D}_1$, 3-fold degenerated level. The absence of detectable ligand-based phosphorescence in the case of the Eu(III) complex as well as the observation of only $^5\text{D}_0 \rightarrow ^7\text{F}_j$ transitions suggests a competitive energy transfer mechanism from the lowest ligand-based triplet state directly to the $^5\text{D}_0$ level. The involvement of the $^5\text{D}_1$ sublevels, however, cannot be precluded.

In order to further characterize the emission of the $[\text{Gd}_9(\text{PLN})_{16}(\text{OH})_{10}]^+$ and $[\text{Eu}_9(\text{PLN})_{16}(\text{OH})_{10}]^+$ complexes, we performed luminescence lifetime measurements in the gas phase. For this purpose, an ensemble of trapped ions was pumped using a gated diode laser until a constant phosphorescence level was reached. The luminescence decay after gating the laser off is very well fitted by a monoexponential decay.

Typical luminescence lifetime measurements for the $[\text{Eu}_9(\text{PLN})_{16}(\text{OH})_{10}]^+$ and $[\text{Gd}_9(\text{PLN})_{16}(\text{OH})_{10}]^+$ complexes are shown in Figure 4. The corresponding luminescence

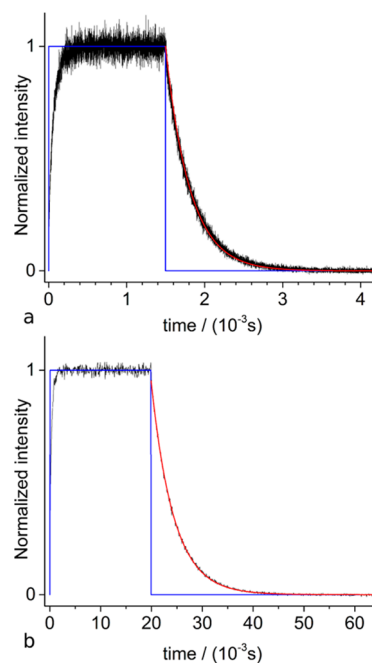


Figure 4. Luminescence lifetime measurements (black) of (a) $[\text{Eu}_9(\text{PLN})_{16}(\text{OH})_{10}]^+$ (445 nm, gated 128 W/cm², 83 K) and (b) $[\text{Gd}_9(\text{PLN})_{16}(\text{OH})_{10}]^+$ (445 nm, gated 128 W/cm², 83 K). The intensity profile of the excitation is indicated in blue. The red curve is a monoexponential fit to the data.

lifetimes at 83 K are $\tau_{\text{Eu}} = 312 \pm 20\ \mu\text{s}$ and $\tau_{\text{Gd}} = 4.4 \pm 0.4\ \text{ms}$, respectively. The more than one order of magnitude longer phosphorescence lifetime measured for the Gd(III) complex supports our interpretation of efficient $(\text{PLN})\text{S}_1 \rightarrow (\text{PLN})\text{T}_1 \rightarrow (\text{Eu(III)})^5\text{D}_0$ energy transfer in the case of the Eu(III) complex at cryogenic temperatures. In contrast, the Gd(III) complex has no such relaxation path available and the PLN-

based triplet state lives correspondingly longer before decaying by phosphorescence.

To conclude, we have reported experimental luminescence measurements on nonanuclear Eu(III) and Gd(III) PLN-hydroxo complexes in the gas phase. We have shown that mass spectrometric techniques allow isolating stoichiometrically pure substances that are unaffected by counterions and that have well-defined charge states. Such measurements are not affected by matrix effects like crystal packing, solvent, or medium polarization effects and, therefore, enable direct comparison with theory. The gas-phase luminescence spectrum of $[\text{Eu}_9(\text{PLN})_{16}(\text{OH})_{10}]^+$ displays emission bands characteristic of Eu(III) in low coordination sites. A more complete analysis of the crystal field splitting for the $[\text{Eu}_9(\text{PLN})_{16}(\text{OH})_{10}]^+$ complex with the support of quantum chemical calculations will be given in a forthcoming paper. From the phosphorescence spectrum of $[\text{Gd}_9(\text{PLN})_{16}(\text{OH})_{10}]^+$, the energy of the ligand-based triplet state was inferred to be $\sim 1000 \text{ cm}^{-1}$ above the emitting level of Eu(III). Corresponding lifetime measurements support the involvement of such a state. Gas-phase measurements like the ones presented here are likely to provide useful information complementary to existing condensed phase probes of molecular lanthanoid emitters because they can unravel heterogeneous broadening and superposition phenomena of various kinds.

■ ASSOCIATED CONTENT

Supporting Information

A description of the synthesis and experimental setup, the emission spectra with abscissa (in cm^{-1}), an ion mobility measurement, a solution spectra of both the Eu(III) and of the Gd(III) compounds, and the coordinates of the $[\text{Eu}_9(\text{PLN})_{16}(\text{OH})_{10}]^+$ structure. This material is available free of charge via the Internet at <http://pubs.acs.org>.

■ AUTHOR INFORMATION

Corresponding Authors

*E-mail: jean-francois.greisch@kit.edu.

*E-mail: detlef.schooss@kit.edu.

Notes

The authors declare no competing financial interest.

■ ACKNOWLEDGMENTS

We acknowledge support from the Deutsche Forschungsgemeinschaft (DFG) as administered by the transregional collaborative research center SFB/TRR 88 "3MET" (C1, C5, and C7). We are also grateful to the Bundesministerium für Bildung und Forschung (BMBF) through the Helmholtz Research Program POF "Science and Technology of Nanosystems" and to the State of Baden-Württemberg for providing the necessary infrastructure.

■ REFERENCES

- (1) Kido, J.; Okamoto, Y. Organo Lanthanide Metal Complexes for Electroluminescent Materials. *Chem. Rev. (Washington, DC, U. S.)* **2002**, *102*, 2357–2368.
- (2) Kuriki, K.; Koike, Y.; Okamoto, Y. Plastic Optical Fiber Lasers and Amplifiers Containing Lanthanide Complexes. *Chem. Rev. (Washington, DC, U. S.)* **2002**, *102*, 2347–2356.
- (3) Fang, J.; You, H.; Chen, J.; Lin, J.; Ma, D. Memory Devices Based on Lanthanide (Sm^{3+} , Eu^{3+} , Gd^{3+}) Complexes. *Inorg. Chem.* **2006**, *45*, 3701–3704.

(4) Mathis, G. Probing Molecular Interactions with Homogeneous Techniques Based on Rare Earth Cryptates and Fluorescence Energy Transfer. *Clin. Chem. (Washington, DC, U. S.)* **1995**, *41*, 1391–1397.

(5) Bunzli, J. C. G.; Piguet, C. Lanthanide-Containing Molecular and Supramolecular Polymetallic Functional Assemblies. *Chem. Rev. (Washington, DC, U. S.)* **2002**, *102*, 1897–1928.

(6) Van Deun, R.; Nockemann, P.; Fias, P.; Van Hecke, K.; Van Meervelt, L.; Binnemans, K. Visible Light Sensitisation of Europium(III) Luminescence in a 9-Hydroxyphenyl-1-one Complex. *J. Chem. Soc., Chem. Commun.* **2005**, 590–592.

(7) Greisch, J. F.; Harding, M. E.; Kordel, M.; Kloppe, W.; Kappes, M. M.; Schooss, D. Intrinsic Fluorescence Properties of Rhodamine Cations in Gas-Phase: Triplet Lifetimes and Dispersed Fluorescence Spectra. *Phys. Chem. Chem. Phys.* **2013**, *15*, 8162–8170.

(8) Greisch, J. F.; Harding, M. E.; Schäfer, B.; Rotter, M.; Ruben, M.; Kloppe, W.; Kappes, M. M.; Schooss, D. Substitutional Photoluminescence Modulation in Adducts of a Europium Chelate with a Range of Alkali Metal Cations: A Gas-Phase Study. *J. Phys. Chem. A* **2014**, *118*, 94–102.

(9) Mironov, V. S. Generalized Superexchange Theory of Fast Energy Transfer, Cooperative Luminescence, and Magnetic Exchange Interactions in Exchange-Coupled Pairs of Lanthanide Ions. *Spectrochim. Acta, Part A* **1998**, *54*, 1607–1614.

(10) Mironov, V. S. Superexchange Mechanism of Energy Transfer between Neighboring Lanthanide Ions in Dielectric Crystals. *Opt. Spectrosc.* **2000**, *88*, 372–376.

(11) Mironov, V. S.; Kaminskii, A. A. The Role of Covalency and Bridging Ligands in Two-Ion Cooperative Optical Transitions in Lanthanide Ion-Coupled Systems. *Phys. Status Solidi B* **2006**, *183*, 481–496.

(12) Mironov, V. S.; Kaminskii, A. A. Covalent Mechanism of Cooperative Optical Transitions in Lanthanide Exchange-Coupled Pairs. Intensity Calculations for Double Transitions in a $\text{M}_2\text{L}_{11} \text{ f}^1\text{-f}^1$ Dimer. *Phys. Status Solidi B* **2006**, *194*, 307–318.

(13) Kordel, M.; Schooss, D.; Neiss, C.; Walter, L.; Kappes, M. M. Laser-Induced Fluorescence of Rhodamine 6G Cations in the Gas Phase: A Lower Bound to the Lifetime of the First Triplet State. *J. Phys. Chem. A* **2010**, *114* (17), 5509–5514.

(14) Becke, A. D. Density-Functional Exchange-Energy Approximation with Correct Asymptotic Behavior. *Phys. Rev. A: At, Mol, Opt. Phys.* **1988**, *38*, 3098–3100.

(15) Gulde, R.; Pollak, P.; Weigend, F. Error-Balanced Segmented Contracted Basis Sets of Double- ζ to Quadruple- ζ Valence Quality for the Lanthanides. *J. Chem. Theory Comput.* **2012**, *8*, 4062–4068.

(16) Schäfer, A.; Horn, H.; Ahlrichs, R. Fully Optimized Contracted Gaussian Basis Sets for Atoms Li to Kr. *J. Chem. Phys.* **1992**, *97*, 2571–2577.

(17) TURBOMOLE, version 6.4; TURBOMOLE GmbH: Karlsruhe, Germany, 2012; available from <http://www.turbomole.com>.

(18) Weigend, F. Accurate Coulomb-Fitting Basis Sets for H to Rn. *Phys. Chem. Chem. Phys.* **2006**, *8*, 1057–1065.

(19) Hubert-Pfalzgraf, L. G.; Miele-Pajot, N.; Papiernik, R.; Vaissermann, J. A Novel Example of Self-Assembly in Lanthanide Chemistry: Synthesis and Molecular Structure of $[\text{Na}(\text{EtOH})_6][\text{Y}_9(\mu_4\text{-O})_2(\mu_3\text{-OH})_8\{\mu\text{-}\eta^2\text{-MeC}(\text{O})\text{CHC}(\text{O})\text{OEt}\}_8\{\eta^2\text{-MeC}(\text{O})\text{CHC}(\text{O})\text{OEt}\}_8]$. *J. Chem. Soc., Dalton Trans.* **1999**, 4127–4130.

(20) Xu, G.; Wang, Z. M.; He, Z.; Lu, Z.; Liao, C. S.; Yan, C. H. Synthesis and Structural Characterization of Nonanuclear Lanthanide Complexes. *Inorg. Chem.* **2002**, *41*, 6802–6807.

(21) Addamo, M.; Bombieri, G.; Foresti, E.; Grillone, M. D.; Volpe, M. Assembling Process of Charged Nonanuclear Cationic Lanthanide(III) Clusters Assisted by Dichromium Decacarbonyl Hydride. *Inorg. Chem.* **2004**, *43*, 1603–1605.

(22) Alexandropoulos, D. I.; Mukherjee, S.; Papatrantaafyllopoulou, C.; Raptopoulou, C. P.; Psycharis, V.; Bekiari, V.; Christou, G.; Stamatatos, T. C. A New Family of Nonanuclear Lanthanide Clusters Displaying Magnetic and Optical Properties. *Inorg. Chem.* **2011**, *50*, 11276–11278.

(23) Petit, S.; Baril-Robert, F.; Pilet, G.; Reber, C.; Luneau, D. Luminescence Spectroscopy of Europium(III) and Terbium(III) Penta-, Octa- and Nonanuclear Clusters with β -diketonate Ligands. *J. Chem. Soc., Dalton Trans.* **2009**, 6809–6815.

(24) Xu, X.; Zhao, L.; Xu, G. F.; Guo, Y. N.; Tang, J.; Liu, Z. A Diabolo-Shaped Dy_9 Cluster: Synthesis, Crystal Structure and Magnetic Properties. *J. Chem. Soc., Dalton Trans.* **2011**, 40, 6440–6444.

(25) Singh-Wilmot, M. A.; Sinclair, R. A.; Andrews, M.; Rowland, C.; Cahill, C. L.; Murugesu, M. Nonanuclear Lanthanide(III) Nanoclusters: Structure, Luminescence and Magnetic Properties. *Polyhedron* **2013**, 53, 187–192.

(26) Richardson, F. S. Terbium(III) and Europium(III) Ions as Luminescent Probes and Stains for Biomolecular Systems. *Chem. Rev. (Washington, DC, U. S.)* **1982**, 82, 541–552.

(27) Blasse, G. Luminescence from the Eu^{3+} ion in D_{4d} symmetry. *Inorg. Chim. Acta* **1988**, 142, 153–154.

(28) Latva, M.; Takalo, H.; Mikkala, V. M.; Matachescu, C.; Rodriguez-Ubis, J. C.; Kankare, J. Correlation between the Lowest Triplet State Energy Level of the Ligand and Lanthanide(III) Luminescence Quantum Yield. *J. Lumin.* **1997**, 75, 149–169.

(29) Sato, S.; Wada, M. Relations between Intramolecular Energy Transfers Efficiencies and Triplet State Energies in Rare Earth β -Diketone Chelates. *Bull. Chem. Soc. Jpn.* **1970**, 43, 1955–1962.

(30) Hebbink, G. A.; Klink, S. I.; Grave, L.; Alink, P. G. B. O.; van Veggel, F. C. J. M. Singlet Energy Transfer as the Main Pathway in the Sensitization of Near-Infrared Nd^{3+} Luminescence by Dansyl and Lissamine Dyes. *ChemPhysChem* **2002**, 3, 1014–1018.

(31) Kleinerman, M. Energy Migration in Lanthanide Chelates. *J. Chem. Phys.* **1969**, 51, 2370–2381.

(32) Yang, C.; Fu, L. M.; Wang, Y.; Zhang, J. P.; Wong, W. T.; Ai, X. C.; Qiao, Y. F.; Zou, B. S.; Gui, L. L. A Highly Luminescent Europium Complex Showing Visible-Light-Sensitized Red Emission: Direct Observation of the Singlet Pathway. *Angew. Chem., Int. Ed.* **2004**, 43, 5010–5013.

(33) Matsuda, Y.; Makishima, S.; Shionoya, S. Intramolecular Energy Transfer in Europium Chelates Due to Excitation of the Triplet State. *Bull. Chem. Soc. Jpn.* **1968**, 41, 1513–1518.

(34) Khalil, G. E.; Thompson, E. K.; Gouterman, M.; Callis, J. B.; Dalton, L. R.; Turro, N. J.; Jockusch, S. NIR Luminescence of Gadolinium Porphyrin Complexes. *Chem. Phys. Lett.* **2007**, 435, 45–49.

(35) Tobita, S.; Arakawa, M.; Tanaka, I. Electronic Relaxation Processes of Rare-Earth Chelates of Benzoyltrifluoroacetone. *J. Phys. Chem.* **1984**, 88, 2697–2702.

(36) Tobita, S.; Arakawa, M.; Tanaka, I. The Paramagnetic Metal Effect on the Ligand Localized $S_1 \rightarrow T_1$ Intersystem Crossing in the Rare-Earth-Metal Complexes with Methyl Salicylate. *J. Phys. Chem.* **1985**, 89, 5649–5654.

(37) Renger, T.; May, V.; Kühn, O. Ultrafast Excitation Energy Transfer Dynamics in Photosynthetic Pigment-Protein Complexes. *Phys. Rep.* **2001**, 343, 137–254.

(38) Telfer, S. G.; McLean, T. M.; Waterland, M. R. Exciton Coupling in Coordination Compounds. *J. Chem. Soc., Dalton Trans.* **2011**, 40, 3097–3108.

(39) Kasha, M. Energy Transfer Mechanisms and the Molecular Exciton Model for Molecular Aggregates. *Radiat. Res.* **1963**, 20, 55–70.

(40) Kasha, M.; Rawls, H. R.; El-Bayoumi, M. A. The Exciton Model in Molecular Spectroscopy. *Pure Appl. Chem.* **1965**, 11, 371–392.